Directing Colloidal Self-Assembly through Roughness-Controlled Depletion Attractions

Kun Zhao[1,2] and Thomas G. Mason[1,2,3,*]

[1]Department of Physics and Astronomy, University of California-Los Angeles, Los Angeles, California 90095, USA
[2]Department of Chemistry and Biochemistry, University of California-Los Angeles, Los Angeles, California 90095, USA
[3]California NanoSystems Institute, University of California-Los Angeles, Los Angeles, California 90095, USA

(Received 29 August 2007; published 28 December 2007)

The surfaces of colloidal particles resulting from many new fabrication methods are not molecularly smooth, so understanding how surface roughness can affect the depletion attraction between the particles and their assembly is very important. We show that the depletion attraction between custom-shaped microscale platelets can be suppressed when the nanoscale surface asperity heights become larger than the depletion agent. In the opposite limit, the attraction reappears and columnar stacks of platelets are formed. Exploiting this, we selectively increase the site-specific roughness on only one side of the platelets to direct the mass production of a single desired assembly: a pure dimer phase.

DOI: 10.1103/PhysRevLett.99.268301 PACS numbers: 82.70.Dd, 05.70.Fh, 47.57.eb, 68.35.Np

Using entropic depletion attractions in particulate dispersions [1–4] to direct the aggregation of a diversity of custom-designed shapes [5–13] is a promising route for creating complex colloidal assemblies. Nanoscale colloids, known as depletion agents, can induce depletion attractions between larger nonspherical particles to form intricate equilibrium phases [14], shape-dependent aggregation [15], and multistep hierarchical assembly dynamics [15,16] in solution. Entropic depletion attractions between colloidal particles are ubiquitous and arise solely from physical considerations of excluded volume. Larger colloidal particles dispersed in a liquid can aggregate when a sufficient concentration of a smaller depletion agent is added [3,4]. As both larger and smaller colloids diffuse in the liquid, the smaller colloids exert an osmotic pressure, Π, on the surfaces of the larger particles. When two larger particles nearly touch, the smaller colloids can become excluded from the region in between them, creating an attractive force due to an imbalance in Π. This attractive force is very short in range, corresponding to the diameter, d, of the depletion agent. For large enough volume fractions, ϕ_s, of the smaller depletion agent, the maximum depth of the potential energy well can become significantly larger than thermal energy, k_BT, leading to slippery diffusion-limited aggregation and even gelation of the larger colloids [17,18]. For smooth, spherical colloids, there is good agreement between the classic theoretical predictions and experiments [1,2].

Hierarchical multistage assembly can arise from slippery depletion attractions between nonspherical colloids [15]. In surfactant micellar solutions, wax microdisks having molecularly smooth faces aggregate face-to-face into columnar stacks. The face-to-face depletion attraction energy at contact between two platelets is $U_{\rm ff} = -V_e\Pi = -(Ad)\Pi$, where V_e is the excluded volume and A is the area of a face. For spherical depletion agents, $\Pi = 6\phi_s k_B T/(\pi d^3)$, and $U_{\rm ff}$ is [15]:

$$U_{\rm ff}(\phi_s, d) = -\left(\frac{6A}{\pi d^2}\right)\phi_s k_B T. \quad (1)$$

Empirically, for ϕ_s such that $U_{\rm ff}/k_BT > 3$, isolated columns of disks form and ultimately grow long enough that the side-side interaction between long columns also becomes larger than several k_BT, causing side-by-side bundling of the columns. Hierarchical aggregation also occurs for rodlike particles [16], although the specific sequence, involving sheets of rods that then unite to form smectic layers, is different.

To explore beyond molecularly smooth particles, we lithographically fabricate polymeric pentagonal platelets out of a clear epoxy photoresist (SU-8) using an i-line Ultratech XLS 5:1 reduction stepper [5]. These monodisperse pentagons are 1 μm thick, have 1.8 μm edge lengths, and are stabilized against aggregation in aqueous solution by *N*-(trimethoxysilylpropyl)-ethylenediamine, triacetic acid trisodium salt. Micelles of sodium dodecylsulfate (SDS) ($d = 4$ nm), fractionated nanoemulsion droplets ($d = 130 \pm 10$ nm—SDS stabilized) [19], and various sizes of monodisperse polystyrene (PS) spheres (20 nm $\leq d \leq$ 140 nm; sulfate stabilized) are used as depletion agents. We mix the depletion agent with a dilute particle dispersion to set ϕ_s and the particle volume fraction ϕ_l, seal the mixture into rectangular microcapillaries, inhibit sedimentation by reorienting the capillaries, and wait at least 24 hours (over 10 times the diffusive doubling period) to ensure that any aggregation, if present, will be detected. To reduce the complexity associated with rapid aggregation, we keep $\phi_l \lll 1$ (typically $10^{-4} < \phi_l < 10^{-3}$). Debye screening lengths associated with charged depletion agents are only a few nanometers and are neglected for simplicity. Atomic force microscopy reveals that the natural distribution of asperity heights on the faces of the platelets [Figs. 1(a) and 1(b)] has an average $h = 17 \pm 7$ nm and a few taller asperities around 30 nm.

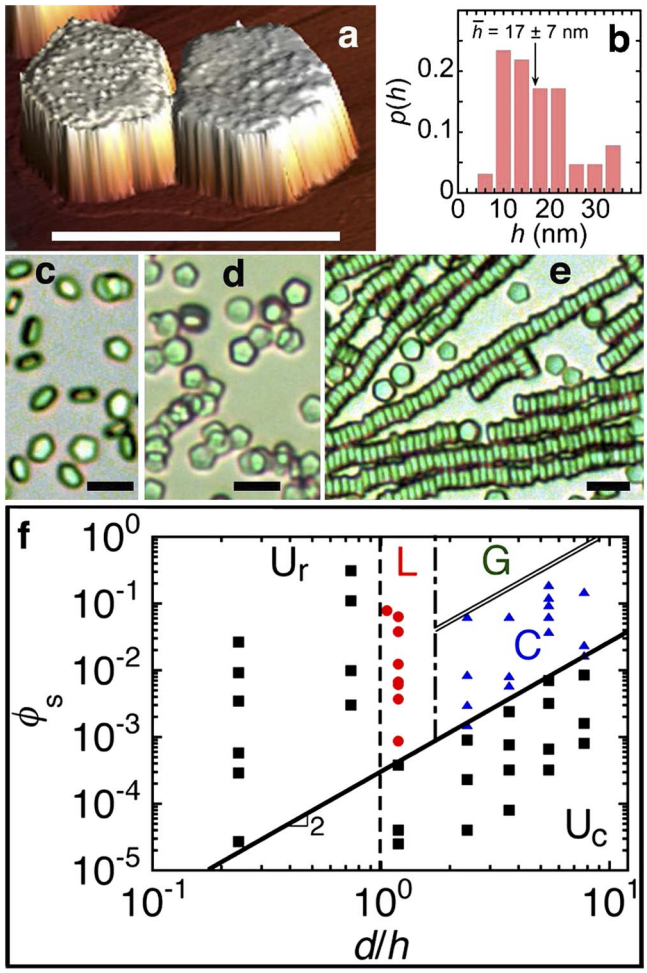

FIG. 1 (color online). Surface roughness-controlled depletion attractions between platelike particles. (a) Atomic force micrographs reveal a distribution of asperities on the flat faces of the pentagons. The height axis has been enlarged twofold to display the surface roughness with greater clarity. (b) Probability distribution of asperity heights $p(h)$ has an average: $h = 17 \pm 7$ nm. (c) Pentagonal polymer platelets in dilute aqueous solution remain unaggregated when the diameter d of the depletion agent is smaller than the average asperity height h (SDS at 20 mM: $d = 4$ nm, $\phi_s = 0.35\%$). Bars are 5 μm. (d) Lateral aggregation of platelets occurs when d/h just exceeds unity (PS spheres: $d = 20$ nm, $\phi_s = 0.067$). (e) Long columnar aggregates are observed for larger d/h and ϕ_s (nanoemulsion: $d = 130$ nm, $\phi_s = 0.15$). (f) Universal aggregation diagram of particles having rough facets at dilute ϕ_l. No aggregation occurs for $d/h < 1$ (region U_r), nor below the solid line of constant attractive energy, $U_{\mathrm{ff}}/(k_BT) = 10$ (region U_c) (squares). Lateral aggregates (L) are observed for $d/h \approx 1$ (circles). Long columns of platelets (C), including side-by-side bundles and T structures of columns, form at higher ϕ_s and d/h (triangles). A disordered gel-like structure (G) of platelets can occur at even larger ϕ_s and d/h.

Optical microscopy observations at different ϕ_s and d/h reveal boundaries associated with aggregation. For $d/h < 1$, the platelets remain unaggregated [Fig. 1(c)]. For $d/h > 1$ and sufficiently high ϕ_s, we find "lateral" aggregate structures [Fig. 1(d)]. The platelets are attracted face-to-face, yet because their centers are highly offset laterally, they do not form straight columns. For d/h well above unity, long columnar stacks of platelets form [Fig. 1(e)]. Within the columns, pentagons tend to align with their vertices in the same direction, yet rotational dynamics is seen within an individual column, since the energy cost to rotate two pentagons out of alignment is less than k_BT. These columns, when long enough, can also aggregate side to side, forming bundles.

From these observations, we create a diagram for roughness-controlled depletion attractions between platelets [Fig. 1(f)]. When asperities are tall (region U_r), smaller depletion agents can still diffuse between faces and inhibit aggregation. However, for $d > h$, the excluded volume relative to k_BT becomes large, leading to lateral and columnar aggregation (regions L and C, respectively). Only a relatively small areal density of asperities having $h > d$ on one of the surfaces is necessary to dramatically reduce the excluded volume and hence strength of the depletion attraction between the surfaces. The solid line, $\phi_s \sim (d/h)^2$, corresponds to $U_{\mathrm{ff}} \approx 10 k_BT$ for smooth faces from Eq. (1); the true aggregation criterion associated with this boundary is closer to $3k_BT$, since asperities will tend to reduce U_{ff} from this ideal limit. Below the solid line (region U_c), ϕ_s is too low for aggregation to occur. T-like configurations of short columns and even highly disordered gels (region G) occur at very large ϕ_s, where side-side and side-face potentials also significantly exceed k_BT.

By increasing the size of pluronic micelles [20–22] through heating to make $d > h$, we can effectively turn on the depletion attraction [23] between particles that have rough surfaces through a mechanism that does not rely on the temperature dependence of ϕ_s. Block copolymer pluronic micelles (P103) have $d < h$ at lower temperature ($d = 15$ nm at $T = 26\,^\circ$C) and have $d > h$ at higher temperature ($d = 34$ nm at $T = 40\,^\circ$C) without creating a large change in the micellar concentration, measured using dynamic light scattering. For sufficiently large ϕ_s, as T is increased so that d exceeds h, the depletion attraction can be effectively turned on. We use 3.75 wt% of P103 in water, much larger than the critical micelle concentration of 0.07 wt% at 26 °C [21]. As shown in Fig. 2, pentagonal platelets aggregate face-to-face to form columns for $T = 40\,^\circ$C, and these reversibly disaggregate into individual platelets as T is cycled back to 26 °C. For $T = 40\,^\circ$C, the distribution of column lengths favors shorter columns [Fig. 2(c)]; as columns grow, the time for them to diffuse and approach end-to-end in order for the faces of the capping pentagons to meet becomes extremely long. Thus, for rapid quenches in which the attractive potential well becomes significantly deeper than thermal energy, the length distribution of the columnar aggregates is primarily governed by kinetics and is not an equilibrium state. In principle, for weaker attractions, it is possible to obtain an equilibrium distribution of short columns in coexistence with a significant monomer population. This thermal method of controlling the

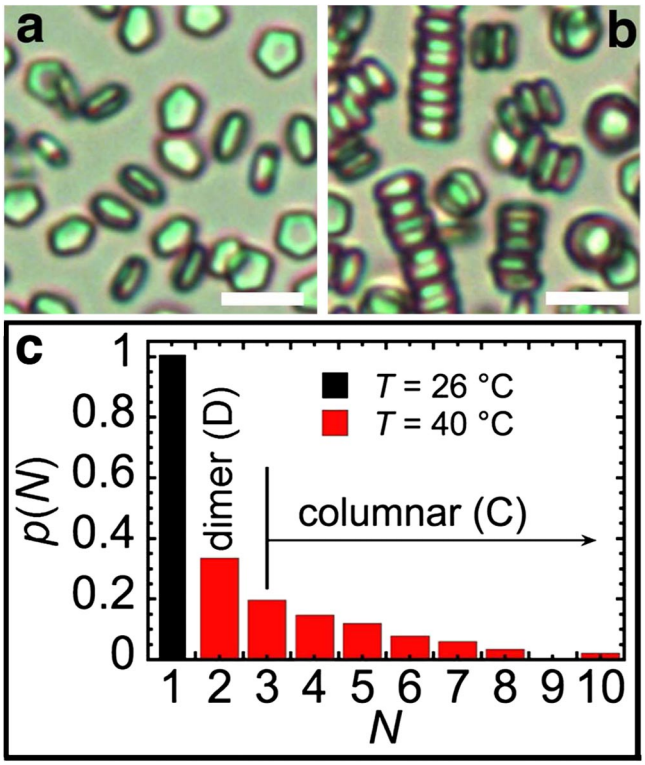

FIG. 2 (color online). Turning on depletion attractions using temperature T to increase the diameter d of the depletion agent. The depletion agent is a pluronic copolymer (P103 by BASF) at 3.75% by mass ($\phi_s \approx 9\%$). Scale bars of optical micrographs are 5 μm. (a) At lower $T = 26\,^{\circ}\mathrm{C}$, $d = 15$ nm and the pentagons remain unaggregated due to roughness ($d < h$). (b) At higher $T = 40\,^{\circ}\mathrm{C}$, $d = 34$ nm and the pentagons aggregate face-to-face into columns ($d > h$). (c) Probability p of observing a column comprised of N pentagons at lower T (first bar) and higher T (other bars).

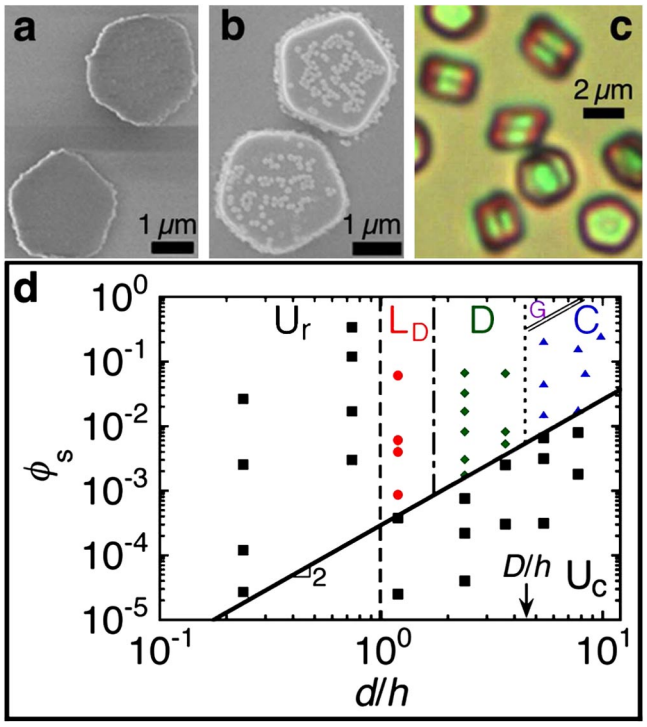

FIG. 3 (color online). Controlling the structure of depletion aggregates by tailoring site-specific surface roughness. Janus platelets are roughened to a higher degree on only one face by binding silica nanospheres (diameter $D = 75$ nm) prior to lift-off from the wafer. Scanning electron micrographs show: (a) The untreated faces have smaller roughness $h \approx 17$ nm. (b) Opposite faces to which silica spheres are bound have greater roughness $D \approx 75$ nm. (c) For $h < d < D$, the silica-modified Janus pentagons form aligned dimers when a depletion agent (PS spheres: $d = 40$ nm at $\phi_s = 0.8\%$) is added (optical micrograph). (d) Phase diagram of assembled structures: unaggregated pentagons (U_r and U_c—squares), offset lateral dimer aggregates (L_D—circles), aligned dimers (D—diamonds), long columnar stacks (C—triangles), disordered gel (G).

depletion-induced aggregation by tuning $d(T)/h$ differs from a method based on changing $\phi_s(T)$ [23] near the critical micelle concentration.

To further test our hypothesis, we tailor the roughness of the pentagons to increase the asperity heights and density. We have deposited uniform PS spheres that have a diameter of $D = 40$ nm over all of the faces and sides of the pentagons, and we have repeated our observations of the aggregation using a variety of depletion agents. We now observe aggregation for $d > D$ at the same ϕ_s. This result is consistent with our hypothesis, since the effective asperity heights have been changed from h to D.

By altering the roughness on specific surfaces of the particles and systematically increasing d, we reveal a method for directing the mass production of one unique assembly in solution. After lithographically fabricating the platelets, but before they are released from the substrate, we increase the roughness of every pentagon by depositing a layer of silica nanoparticles with $D = 75$ nm at about 20% areal density on only the top and side surfaces of each platelet. This provides two-faced pentagons that are Janus particles [24] in the sense of nanoscale surface roughness: one side has roughness D and the other side has roughness h. As shown in Fig. 3, when $d < h < D$, no aggregation occurs at any ϕ_s (region U_r). For d/h just larger than unity, offset face-to-face lateral aggregates of two particles are formed (region L_D). Above this, for $h < d < D$, we find a new regime in which we form an equilibrium dimer phase of two aligned pentagons [Fig. 3(c) and region D in Fig. 3(d)]; no long columns form and monomers are essentially not present. The aligned dimers form when the two smoother surfaces of two Janus platelets aggregate face-to-face, exposing the rougher surfaces that cannot aggregate. For $h < D < d$, the hierarchical columnar aggregation and subsequent bundling is observed (region C), as in Fig. 1.

The general problem of how surface roughness affects the strength and range of the depletion attraction is interesting and rich. The strength of the depletion attraction between two rough faces is generally smaller compared to

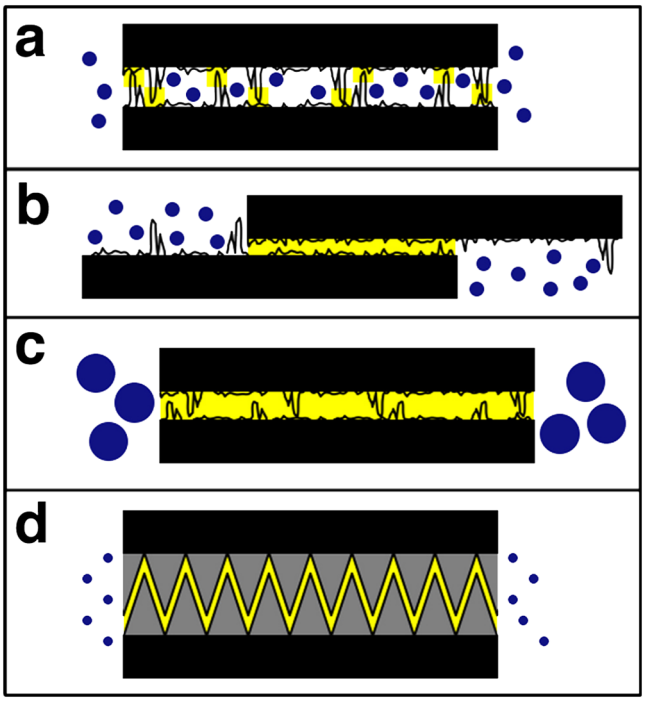

FIG. 4 (color online). Asperities influence the excluded volume (shaded regions—yellow) of the depletion agent (solid circles—blue) between platelets. (a) Particles having asperities with height $h > d$ on the surfaces can greatly reduce the excluded volume between aligned plates, inhibiting aggregation. (b) Thermal rearrangement can still lead to laterally offset face-to-face aggregation in which the largest asperities on one surface avoid contact with the opposite surface. (c) When $d > h$, the excluded volume becomes large, leading to columnar aggregation. (d) In principle, ideally corrugated surfaces, such as a sawtooth pattern, can create larger excluded volumes and stronger depletion attractions than just simple flat surfaces.

the perfectly smooth limit due to the reduction in excluded volume [Fig. 4(a)]. An encounter of two faces in a perfectly aligned configuration is improbable, so particles will usually approach each other out of alignment. The particles can still aggregate face-to-face but may remain laterally offset in a way that maximizes the excluded volume subject to the constraints introduced by the asperities [Fig. 4(b)]. This offset "lateral" aggregation would be precluded by a uniform height distribution of noninterlocking asperities that densely cover the faces. When $d > h$, the excluded volume is large and the depletion attraction can cause aligned aggregation [Fig. 4(c)]. A periodic triangular distribution of surface asperities that interlock could actually increase V_e [Fig. 4(d)], making U_{ff} larger than what it would be between two perfectly flat surfaces. In the idealized case of surfaces having matching sawtooth grooves, U_{ff} would be enhanced by the ratio of the surface area of the corrugated face divided by the surface area of the perfectly flat face.

We anticipate that a full theoretical treatment of roughness-controlled depletion attractions will refine our basic explanation. Considering how different probability distributions of the asperity positions and heights on the surfaces can affect the potential between flat and curved surfaces would be interesting. Likewise, simulations that incorporate such roughness distributions could generate ensembles of particles that mimic actual dispersions and would provide a means of determining how variations in roughness, especially for very tall asperities, can affect the aggregation.

Controlling the spatial distribution and heights of asperities on custom-shaped colloids is a promising route for creating complex assemblies comprised of many parts. By adding depletion agents from smaller to larger sizes, or by changing the temperature to increase d, it is possible to mass-produce unique desired assemblies by tailoring site-specific roughness on different surfaces of custom-shaped colloids. This approach, in combination with designing the surface areas of flat facets and controlling ϕ_s, can provide precise control over many stages of directed aggregation.

This work has been supported in part by the National Science Foundation (No. CHE0450022) and the McTague Chair.

*Corresponding author.
mason@physics.ucla.edu

[1] Y. N. Ohshima *et al.*, Phys. Rev. Lett. **78**, 3963 (1997).
[2] D. Rudhardt, C. Bechinger, and P. Leiderer, Phys. Rev. Lett. **81**, 1330 (1998).
[3] S. Asakura and F. Oosawa, J. Chem. Phys. **22**, 1255 (1954).
[4] S. Asakura and F. Oosawa, J. Polym. Sci. **33**, 183 (1958).
[5] C. J. Hernandez and T. G. Mason, J. Phys. Chem. C **111**, 4477 (2007).
[6] S. Badaire *et al.*, J. Am. Chem. Soc. **129**, 40 (2007).
[7] D. Dendukurl *et al.*, Nature Mater. **5**, 365 (2006).
[8] J. P. Rolland *et al.*, J. Am. Chem. Soc. **127**, 10 096 (2005).
[9] M. Sullivan *et al.*, J. Phys. Condens. Matter **15**, s11 (2003).
[10] J. C. Love *et al.*, Langmuir **17**, 6005 (2001).
[11] A. B. D. Brown, C. G. Smith, and A. R. Rennie, Phys. Rev. E **62**, 951 (2000).
[12] M. D. Hoover, J. Aerosol Sci. **21**, 569 (1990).
[13] L. Manna *et al.*, Nature Mater. **2**, 382 (2003).
[14] M. Adams *et al.*, Nature (London) **393**, 349 (1998).
[15] T. G. Mason, Phys. Rev. E **66**, 060402 (2002).
[16] Z. Dogic, Phys. Rev. Lett. **91**, 165701 (2003).
[17] J. N. Wilking *et al.*, Phys. Rev. Lett. **96**, 015501 (2006).
[18] A. D. Dinsmore *et al.*, Phys. Rev. Lett. **96**, 185502 (2006).
[19] T. G. Mason *et al.*, J. Phys. Condens. Matter **18**, R635 (2006).
[20] P. Alexandridis and T. A. Hatton, Colloids Surf. A **96**, 1 (1995).
[21] P. Alexandridis, J. F. Holzwarthf, and T. A. Hatton, Macromolecules **27**, 2414 (1994).
[22] S. L. Nolan *et al.*, J. Colloid Interface Sci. **191**, 291 (1997).
[23] J. R. Savage *et al.*, Science **314**, 795 (2006).
[24] C. Casagrande *et al.*, Europhys. Lett. **9**, 251 (1989).